JOURNAL OF GUIDANCE, CONTROL, AND DYNAMICS
Vol. 16, No. 4, July–August 1993

Linear Quadratic Gaussian/Loop Transfer Recovery Design for a Helicopter in Low-Speed Flight

Jeremy J. Gribble*
University of Glasgow, Glasgow G12 8QQ, Scotland, United Kingdom

A control law for a helicopter in low-speed flight is designed using the linear quadratic Gaussian/loop transfer recovery method. The specifications are adapted from a subset of the U.S. Army helicopter handling qualities requirements. The design model consists of the rigid-body dynamics linearized about the 30 kt forward flight condition, together with a simplified, low-order representation of actuator and rotor dynamics. Evaluation is performed using higher-order models, obtained by linearization about several different points in the flight envelope, covering the speed range from 10 to 50 kt. These models contain more accurate representations of the high-frequency actuator and rotor modes. The final selection of the numerical values of the linear quadratic parameters is made by numerical optimization of the loop shape. It is found that the specifications considered can be satisfied for all of the evaluation models without gain scheduling.

Introduction

THE publication of updated U.S. Army helicopter handling qualities requirements[1] has prompted interest within the rotorcraft community of a re-examination of multivariable control law design methods (see, for example, Garrard et al.[2] and Walker and Postlethwaite[3]). This is because the improved agility of modern aircraft has resulted in increased cross-coupling between channels so that classical single-input/single-output (SISO) techniques may no longer be adequate. This paper presents a case study of the linear quadratic Gaussian/loop transfer recovery (LQG/LTR) method[4,5] applied to the helicopter flight control problem with the intention of examining the method for this particular application. The paper attempts to show how the design process is driven by the characteristics of the vehicle and the specifications. As an alternative to formal analytical loop shaping,[4] the final choice of the numerical values of the linear quadratic weighting parameters is made from the numerical solution of a singular value loop shaping problem.

The system considered in this paper is a typical combat rotorcraft. An account of the main facts about rotorcraft dynamics at an introductory level may be found in McLean.[6] The work described here is based on linearization of a generic nonlinear helicopter model called HELISTAB.[7] The most detailed model used here contains representations of the rigid-body modes, the actuator, and rotor flapping dynamics. One of the factors which makes helicopter flight control system (FCS) design difficult is the relatively small frequency separation between the rigid-body modes on one hand, and actuator and rotor effects on the other.[8] In addition to the rotor flapping modes already mentioned, the rotors of an actual vehicle will have lead-lag dynamics. Although it is acknowledged that the lead-lag dynamics are of importance, the models available did not include these effects, and they have not been considered here. However, if the lead-lag dynamics manifest themselves at low frequencies as phase lags, then it should be possible to include them within the framework presented here without any increase in the complexity of the resulting controller.

An earlier and very detailed study of the application of linear quadratic optimal methods to the helicopter FCS problem is due to Hofmann et al.[9] The approach described in this reference is rather different from that in the present work, being concerned with the LQG/LQR framework in a more "traditional" way as a means of providing estimated full state feedback in the presence of sensor noise. Furthermore, this reference predates the publication of the revised handling qualities specifications.[1]

Received March 11, 1992; revision received May 29, 1992; accepted for publication Aug. 25, 1992.

*Lecturer, Department of Electronics and Electrical Engineering.

Specifications

The helicopter is a multirole vehicle whose control system requirements are a function of the handling qualities task being carried out. Different handling qualities tasks are associated with different ranges of speed. In this paper we will consider a design for the low-speed range (15–45 kt) with the following selection of specifications taken from Ref. 1. (Brief and/or simplified explanations of the specifications are given for the benefit of readers who do not have ready access to Ref. 1 or its draft version Hoh et al.[10])

1) Pitch, roll, and heading should exhibit rate command and attitude/heading hold characteristics.[1] Broadly speaking, "rate command" implies that the aircraft's attitude/heading monotonically diverges from trim following a step command. A "hold" characteristic implies that the aircraft's attitude/heading should return to within 10% of its peak excursion from trim within 10 s following an impulse directly to the appropriate control actuator.

2) The bandwidth and phase delay of the pitch and roll angles in response to pilot input should satisfy the requirements of section 3.3.2.1 of Ref. 1. The bandwidth is defined with respect to the frequency domain characteristics of the outer feedback loop closed around the aircraft by the pilot. The definition is intended to capture the greatest speed of response that can be obtained without any tendency toward pilot induced oscillations. In the simplest case the bandwidth is the frequency at which the phase lag between the pilot's input and the pitch or roll is -135 deg. This bandwidth should exceed 2.0 rad/s for pitch and 3.5 rad/s for roll. The phase delay is related to the slope of the closed-loop frequency response beyond the bandwidth frequency and is a measure of the effective time delay experienced by the pilot.

3) Pitch and roll mid-term response: the effective damping ratios should be greater than 0.35.[1] Since Ref. 1 does not seem to contain a definition of the effective damping ratio, values were obtained by performing a least squares fit of the pitch and roll impulse responses (or equivalently, the pitch rate and roll rate step responses) to those obtained for the transfer function

$$b\omega_n^2\,(as + 1)/s(cs + 1)(s^2 + 2\zeta\omega_n s + \omega_n^2)$$

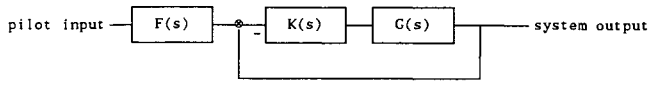

Fig. 1 Block diagram of control law structure: $G(s)$ = plant, $K(s)$ = Kalman filter-based compensator, and $F(s)$ = shaping filter.

The pole at the origin gives a rate command response, the quadratic factor in the denominator represents a dominant oscilliatory mode, and the remaining linear factors approximate the effects of the rest of the modes. The effective damping ratio was taken to be the value of ζ.

4) Short term pitch, roll, and yaw response to disturbance inputs[1]: This is similar to requirement 2 except that the inputs are injected directly to the control surface actuators. The response type for such inputs is of the attitude command type rather than rate command, and this modifies the calculation of the bandwidth and phase delay slightly.

5) Heading bandwidth and phase delay in response to pilot input[1]: This is the same as requirement 2, where the heading bandwidth should exceed 3.5 rad/s.

6) Mid-term heading response[1]: This is similar to requirement 3.

7) Coupling requirements: yaw due to collective[1] and pitch-to-roll and roll-to-pitch coupling[1,10]—following a step command on height rate, the yaw rate after 1 and 3 s should not exceed certain values. Following a step command on the pitch (roll) channel, the off-axis rate should not exceed 25% of the desired on-axis rate for at least 4 s. Note that the draft version of this requirement has been retained from Hoh et al.[10] since the earlier version appears to be more readily applicable to rate command systems than the revised version.

8) Height rate response to a step input[1]: This should resemble a delayed first-order response with a time constant less than 5 s, and a time delay less than 0.20 s. The parameters are determined by a least squares fit. The requirements just quoted are limited to those for small amplitude changes in flight condition as is appropriate for linear design.

Summary of the Linear Quadratic Gaussian/Loop Transfer Recovery Methodology

In this section we will summarize the basic LQG/LTR method to establish notation. The treatment will follow that given in Maciejowski.[5] The final control law has the structure shown in Fig. 1. The system to be controlled is represented by the transfer function (matrix) $G(s)$ and there is cascade compensation $K(s)$. The multivariable feedback loop is closed around the transfer function $G(s)K(s)$. A shaping filter $F(s)$ is used outside the loop. The LQG/LTR method is relevant only to the design of $K(s)$; the design of the shaping filter is discussed later.

The starting point is a linear state space model of a dynamic system which is excited by process noise w and measurement noise v in addition to the control input u

$$x' = Ax + Bu + \Gamma w \tag{1a}$$

$$y = Cx + v \tag{1b}$$

The noise terms w and v are zero-mean Gaussian white noise vectors with covariance matrices W and V, respectively, for which the associated Kalman filter gain matrix K_{lqe} can be found. A full state feedback matrix, K_{lqr}, for the linear quadratic regulator problem is obtained by specifying state and input weighting matrices Q and R, respectively. The compensator $K(s)$ can then be written in state space form as the well-known combination of Kalman filter with estimated state variable feedback

$$u = K_{lqr}x_{est} \tag{2a}$$

$$x' = (A - BK_{lqr} - K_{lqe}C)x_{est} + K_{lqe}y \tag{2b}$$

where x_{est}, the compensator state vector, is also an estimate of the system state vector x. In the absence of a reference signal the compensator input is the system output y, and the compensator output is the system input u. The LQG/LTR method exploits the asymptotic properties of the LQG/LQR controller already given, to simplify the design process by breaking it down into the following two stages.

Stage 1: Choose Γ, W, and V so that the transfer function $C(sI - A)^{-1}K_{lqe}$ has properties which would be satisfactory for the actual loop transfer function $G(s)K(s)$.

Stage 2: Set $Q = C'C$ and $R = \rho I$ where ρ is a scalar parameter. Then, provided certain conditions are satisfied, the actual loop transfer function $G(s)K(s)$ recovers the transfer function found in stage 1 in the limit $\rho \to 0$.

The parameters Γ, W, and V can be chosen on the basis of singular value loop shaping.[11] Stage 2 is then a robustness recovery procedure, with the choice of ρ being dictated (in principle) by a tradeoff between recovery of the nominal loop shape and sensitivity to noise, the latter being associated with the 40 dB/decade rolloff of the LQG/LQR controller being pushed to higher and higher frequencies as ρ is decreased.

We follow Maciejowski[5] in extending the formalism to allow for the possibility of colored process noise, so that the process noise term is not itself white, but is the output of a linear dynamic system driven by white noise term u_w. The plant model is

$$x_p' = A_p x_p + B_p u_p + \Gamma_p y_w \tag{3a}$$

$$y_p = C_p x_p + v \tag{3b}$$

The process noise dynamics are

$$x' = A_w x_w + B_w u_w \tag{4a}$$

$$y_w = C_w x_w + D_w u_w \tag{4b}$$

and the intensities of the white noise terms v and u_w are now

$$E(vv') = V,\ E(u_w u_w') = W \tag{5}$$

The plant and process noise dynamics can be combined as:

$$\begin{bmatrix} x_p' \\ x_w' \end{bmatrix} = \begin{bmatrix} A_p & \Gamma_p C_w \\ 0 & A_w \end{bmatrix} \begin{bmatrix} x_p \\ x_w \end{bmatrix} + \begin{bmatrix} B_p \\ 0 \end{bmatrix} u_p + \begin{bmatrix} \Gamma_p D_w \\ B_w \end{bmatrix} u_w \tag{6a}$$

$$y_p = \begin{bmatrix} C_p & 0 \end{bmatrix} \begin{bmatrix} x_p \\ x_w \end{bmatrix} + v \tag{6b}$$

This augmented plant model can be written in the form of Eqs. (1) with the identifications

$$A = \begin{bmatrix} A_p & \Gamma_p C_w \\ 0 & A_w \end{bmatrix}, \qquad B = \begin{bmatrix} B_p \\ 0 \end{bmatrix}$$

$$\Gamma = \begin{bmatrix} \Gamma_p D_w \\ B_w \end{bmatrix}, \qquad C = \begin{bmatrix} C_p & 0 \end{bmatrix} \tag{7}$$

We see that the feedback controller $K(s)$ is determined by the complexity of the helicopter design model (A_p, B_p), the system outputs (C_p), the coupling of the process noise into the plant model (Γ_p), the process noise model (A_w, B_w, C_w, D_w), the noise intensities (W, V), and the LQG/LTR recovery parameter ρ.

Finally, we note that the LQR problem associated with Eq. (7) appears to present some difficulty since the noise states x_w are uncontrollable from the plant input. (It is not that we want to control these states, but we need to find the state feedback matrix from them to the plant input.) This difficulty can be overcome by partitioning the appropriate Riccati equation and ignoring the portion associated with the uncontrollable dynamics.[12]

Design of the Feedback Loop

The design of the feedback loop reduces to making a series of choices for the parameters A_p, B_p, Γ_p, etc. We will examine these choices in turn, starting with the system output (C_p). The standard version of the LQG/LTR formalism is limited to square systems, and since the helicopter has four inputs, we can control four outputs. The selection of outputs was height rate, pitch angle, roll angle, and heading. (Heading was included because of the assumption of the heading hold requirement.) Rate command response types are then obtained by using a shaping filter outside the feedback loop. Since height rate is measured in feet/second, and the attitudes in radians, scaling of the outputs was introduced to improve the numerical conditioning of the problem. The scaling factors were height rate: 10 ft/s, pitch: 0.1 rad, roll: 0.2 rad, and heading: 0.2 rad. The relative scaling of pitch, roll, and heading was chosen to reflect the requirements for minimum achievable angular rates for aggressive maneuvering at "level 1" cited in table 1(3.3) of Ref. 1. In conjunction with the choice of plant model (A_p, B_p) these outputs, together with their scale factors, determine the output matrix C_p.

We now consider the choice of the plant dynamic model. The HELISTAB nonlinear helicopter model contains representations of the rigid-body, actuator, and rotor flapping modes. The LQG/LTR method assumes a linear plant model. In the first place, since we are concerned with the low speed range 15-45 kt, we choose to linearize about the 30-kt flight condition in the center of this range. Clearly, the design model must include the rigid body states. In deciding how much more detail to include, a tradeoff must be made between two factors. The order of the compensator in Eq. (2) is the same as that of the augmented system. A very detailed plant model will perhaps lead to a good nominal performance, but the controller will be of very high order. Conversely, a model with less detail will give a lower-order compensator, but possibly at the cost of poorer performance.

To assess the level of detail needed, we follow Tischler[8] and model the effects of the actuator and rotor dynamics as pure time delays at the system inputs. Numerical values were obtained by comparing the open-loop frequency response of the rigid-body model to that of the full linearized model including actuators and rotor flapping. The values obtained were from collective to height rate, 0.064 s; from longitudinal cyclic to pitch angle, 0.138 s; from lateral cyclic to roll angle, 0.117 s; and from tail rotor collective to heading angle, 0.037 s.

As we will see later, the design gain crossover frequency used was 4.0 rad/s. At this frequency the phase lag associated with the delays in the pitch channel (the worst case) is approximately 32 deg. It seemed unrealistic to ignore an effect of this size, therefore, the ninth-order rigid-body helicopter model was augmented by first-order SISO Padé approximations for the time delays at each of the four inputs. So, for example, to the first input of the rigid-body model was attached the SISO system $(1-0.5s\tau)/(1+0.5s\tau)$ with $\tau = 0.064$, and similarly for the remaining three input-output pairs. Thus the plant model (A_p, B_p) is of order 13, the first four states being the time delay state variables, and the remaining nine being the rigid-body state variables. (The rigid-body and time delay state space models are given in the Appendix.)

We now consider the choice of the process noise dynamics (A_w, B_w, C_w, D_w) and the coupling matrix Γ_p. The most obvious choice for Γ_p is to make it equal to the helicopter design model input matrix B_p. However, this assumes that the disturbance inputs enter the system in the same way as the control inputs. Even though the process noise is used as a design parameter rather than as a model of a physical effect, it was felt to be more appropriate to choose the structure of Γ_p to reflect the way in which disturbances arise physically. Disturbances in the height rate, attitudes, and heading are caused by components of disturbing force and torque which determine the time derivatives of height rate and angular velocity. Therefore, the elements of Γ_p coupling the four components of y_w to the time derivatives of the body axis vertical velocity and the angular velocity components were set to 1, all remaining elements being set to 0. The small discrepancy between height rate and body axis vertical velocity was ignored. Explicitly, Γ_p is a sparse 13×4 matrix whose only nonzero elements are

$$\Gamma_p(6, 1) = \Gamma_p(7, 2) = \Gamma_p(10, 3) = \Gamma_p(12, 4) = 1 \qquad (8)$$

The process noise dynamics can be used to obtain a form of integral action.[5] The simplest way of doing this is to take $A_w = D_w = [0]$ and $B_w = C_w = I$ where I and $[0]$ are the 4×4 identity and zero matrices, respectively. Thus there is a SISO integration between each component of the source white noise u_w and the corresponding component of the colored noise y_w. Therefore, the controller will reject steady disturbances on each of the four channels, which in classical control implies integral action.

The selection of the 4×4 noise covariance matrices W and V is the most difficult stage of the whole design. W and V are chosen to be diagonal on the grounds of simplicity. Since W and V can both be multiplied by the same factor without affecting the solution of the Kalman filter Riccati equation, one element, $V(1, 1)$ say, can be fixed leaving seven numerical values to choose. The singular value loop shaping paradigm of Doyle and Stein[11] provides a basis for the choice of these numerical values. Thus, we aim to keep the smallest singular value $\sigma_{\min}$ of the loop transfer function $G(s)K(s)$ large at low frequencies to ensure good tracking, and keep the largest singular value $\sigma_{\max}$ small at high frequencies for robustness and noise rejection. A corollary of these aims is that the largest and smallest singular values should be close in the crossover region.

We recall that W and V can be used to manipulate the loop shape obtained at stage 1 of the LQG/LTR procedure, and that the high-frequency rolloff of this loop shape is 20 dB/decade. Then, the following procedure suggests itself. Choose a SISO "target loop shape" with a 0 dB gain crossover frequency ω_{gc}. Then choose W and V so as to 1) maximize the mean difference (measured in decibels) over the frequency between $\sigma_{\min}[G(j\omega)K(j\omega)]$ and the target loop shape for frequencies below ω_{gc}, subject to the constraint that 2) the mean difference (measured in decibels) over the frequency between $\sigma_{\max}[G(j\omega)K(j\omega)]$ and the target loop shape is zero for frequencies above ω_{gc}.

The SISO transfer function used to generate the target loop shape was taken to be $\omega_{gc}/(s + 0.1\omega_{gc})$. This form was chosen so that the rolloff above ω_{gc} was 20 dB/decade matching that of the transfer function obtained in the first stage of the LQG/LTR procedure. This choice of loop shape implies a minimum desirable loop gain of 20 dB at low frequencies to achieve some reduction of sensitivity to model error.

The choice of the value of ω_{gc} was motivated by the fact that the main advantage of negative feedback control, insensitivity to model error, is obtained at frequencies up to about ω_{gc}. Since we are aiming for handling qualities bandwidths in excess of 3.5 rad/s for roll and heading, then ω_{gc} should exceed this value. On the other hand, if ω_{gc} is too large then it is likely that there would be problems with model error and excessive control action. The value chosen was 4.0 rad/s.

A finite frequency range from 0.01 to 100 rad/s was used for practical reasons. The precise values of the upper and lower limits were not believed to be critical, given that ω_{gc} was not close to either limit. It was found to be very easy to choose W and V manually to get the loop shape very roughly right. A numerical optimization routine was then found to be very effective in fine tuning the loop shape according to the criteria already given. The final values obtained were

$$W(1, 1) = 5.81 \times 10^3, \qquad W(2, 2) = 7.66$$

$$W(3, 3) = 1.06 \times 10^2, \qquad W(4, 4) = 1.08 \times 10^1$$

$$V(1, 1) = 1, \qquad V(2, 2) = 2.47$$

$$V(3, 3) = 4.91 \times 10^{-1}, \qquad V(4, 4) = 1.97$$

Figure 2 depicts the target loop shape and the optimized stage 1 loop shape for the design model. It can be seen that σ_{min} is comfortably above the target value for frequencies up to about 1 rad/s. The variation of σ_{max} follows that of the target loop shape closely for frequencies above 5 rad/s. The difference between the two singular values near the gain crossover frequency is about 2 or 3 dB.

The final parameter in the design of the feedback loop is the recovery parameter ρ. It was noted earlier that as the recovery parameter ρ is decreased, the robustness of the resulting closed-loop system improves at the cost of increased sensitivity to high-frequency noise. In the absence of any specific requirements for noise sensitivity in the handling qualities specifications, the most sensible approach seemed to be to increase ρ to the point of diminishing returns of robustness recovery. Robustness was assessed by consideration of the frequency variation of $\sigma_{min}[I + G(j\omega)K(j\omega)]$ and $\sigma_{min}[I + K(j\omega)G(j\omega)]$. It is well-known[13] that the minimum values of these quantities can be interpreted in terms of conservative gain and phase margins against variations at the plant output and input, respectively. It was found that relatively little increase in the margins was obtained for values of ρ below 0.001, which was the final value used. The lesser of the two margins was close to 0.58 for loop breaking at the plant input. The margin for loop breaking at the plant output was slightly larger (about 0.62) as expected, since the loop shaping was performed at this point.

Design of the Shaping Filter

The preceding section has dealt with the design of the negative feedback loop. So far, little use has been made of specific handling qualities specifications. This is because the only specifications that pertain solely to the feedback loop are the requirements for attitude and heading hold, and the short-term response for disturbance inputs. Apart from influencing the choice of outputs, these specifications have had little influence on the design apart from motivating the choice of gain crossover frequency.

We now consider how the control structure must be modified by the addition of a diagonal shaping filter outside the loop [$F(s)$ in Fig. 1] to address those specifications that do relate to pilot input. Since the error signal is formed directly at the outputs, and since it is desired to control these outputs independently, the simplest strategy is to use four SISO shaping filters to inject command signals into the negative feedback loop at the summing junction. Of course, there might be

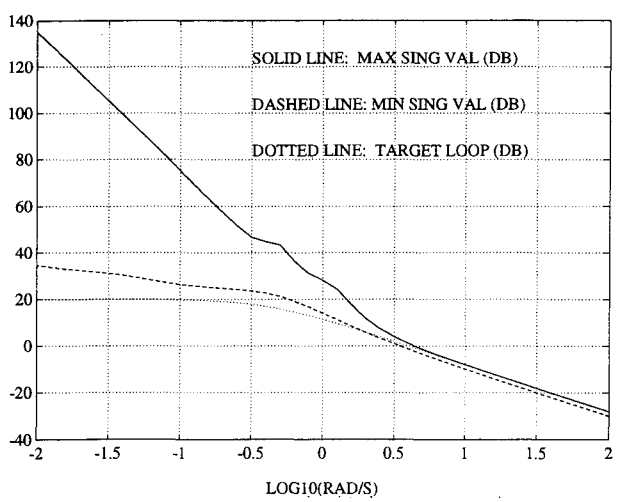

Fig. 2 Maximum and minimum singular values of stage 1 loop shape.

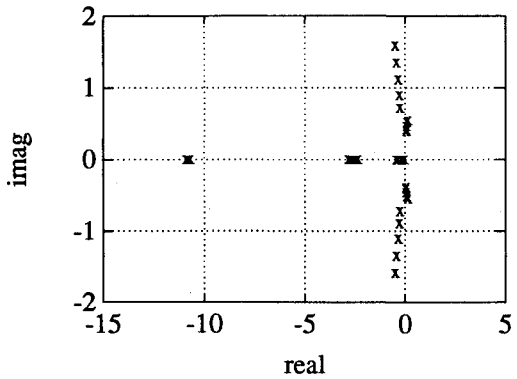

Fig. 3 Open-loop poles of rigid-body modes for 10–50 kt.

circumstances in which one might wish to use a nondiagonal shaping filter at the onset; one example would be if the specifications were modified to include turn coordination.

The first component of the output vector is height rate. The shaping filter was taken to be $(1 + s/4)/(1 + s/0.4)$. The numerator approximately cancels the closed-loop dynamics without the shaping filter in Fig. 1, and the denominator provides a much slower "model" response with a time constant of 2.5 s. As a byproduct, high-frequency inputs are attenuated relative to low-frequency inputs by a factor of 10, which helps to reduce undesired coupling of height rate commands into the other channels. (In principle this could also be done by using crossfeeds within the shaping filter, a point to which we will return.)

We now consider the design of the shaping filters for the control of pitch, roll, and heading. The method used was the same in all three cases, so only the pitch channel will be discussed in detail.

It is desired to have a *rate* command response type. Given that the loop is closed around pitch angle, rather than pitch rate, the most obvious way of achieving this is to use a pure integrator $1/s$ as a shaping filter. However, the extra phase lag of -90 deg at all frequencies would lead to a poor handling qualities bandwidth. To boost the handling qualities bandwidth above 2.0 rad/s, the shaping filter was taken to be of the form

$$(1/s + k_p) = (1 + k_p s)/s \tag{9}$$

so that the filter now has a zero at $s = -1/k_p$ as well as a pole at the origin. This is a trim rate follow-up system since the k_p term dominates on the short time scale, and the pure rate response is only evident in the steady state. The choice of a value for k_p is, as usual, the result of a tradeoff. A very small value would lead to a "pure" rate command response, but the handling qualities bandwidth would be too low. A very large value would give a high handling qualities bandwidth, but the response type would tend to be of the attitude-command type. The implication is that k should be chosen to be the smallest value that gives an acceptable handling qualities bandwidth. It was decided to aim for a handling qualities bandwidth of 2.5 rad/s in pitch and 4.0 rad/s in roll and heading for the design model.

In practice, the attitude frequency responses of the design model were found to be "phase limited." In such cases the definition of the handling qualities bandwidth simplifies to being the frequency at which the phase lag from the pilot's inceptor to the pitch response is 135 deg. Thus, k_p could be chosen to satisfy

$$\angle [1/s + k_p]_{s=2.5j} + \begin{bmatrix} \text{phase of closed-loop system} \\ \text{without shaping filter at 2.5 rad/s} \end{bmatrix} = -135 \text{ deg} \tag{10}$$

Table 1 Selected handling qualities measures

Handling qualities measure		10 kt	20 kt	30 kt	40 kt	50 kt
Handling qualities bandwidth, rad/s	θ	2.6	2.6	2.6	2.6	2.6
	ϕ	5.3	5.3	5.2	5.2	5.2
	ψ	4.2	4.0	3.9	4.4	5.3
Effective damping ratio	θ	0.56	0.58	0.60	0.59	0.57
	ϕ	1.4	1.4	0.95	0.95	0.95
	ψ	0.60	0.60	0.62	0.69	0.74
Pitch-to-roll coupling		0.14	0.17	0.21	0.23	0.24

The positions of the zeros of the attitude shaping filters came out to be -194, -5.43, and -8.00 rad/s for pitch, roll, and heading, respectively.

Evaluation

The helicopter model on which the design was based was the 30-kt forward flight rigid-body model, with SISO time delays placed at each of the four inputs as a crude representation of the effects of actuators and rotors. The evaluation was based on linear models that were extended beyond the design mode in the following two respects:

1) The representation of the actuators was the fullest one available from the linearized HELISTAB model; i.e., nine rigid-body states + four actuator states + six rotor flapping states. The actuators were represented as first-order lags with poles at -12.6 rad/s except for the tail rotor collective pitch whose pole is at -25.0 rad/s. The six rotor states correspond to the coning, advancing flap, and regressing flap modes with poles at about $-9 \pm 10j$, $-16 \pm 36j$, and $-16 \pm 70j$ rad/s.

2) The evaluation was performed not only at 30 kt, but also at 10, 20, 40, and 50 kt. (Since the linearized dynamics of the helicopter vary with velocity, this is a first step toward using the full nonlinear model.) Note that in all five cases, the controller used was the one obtained from the 30-kt design model. There was no gain scheduling.

The performance was evaluated by using frequency and time domain simulations and calculating predicted bandwidths, phase delays, effective damping, etc. These were compared with the requirements of the specifications given earlier with further reference to Ref. 1 where appropriate. All of the predicted handling qualities came out at level 1 on the simplified Cooper-Harper scale,[1] i.e., "satisfactory without improvement." Since it would be impractical to attempt to reproduce all of the data here, a selection will be made to highlight some points of interest. Note that Figs. 4 and 7 used scaled outputs.

Figure 3 shows the variation with flight condition of the open-loop poles of the rigid-body model. The main feature is that the Dutch roll mode becomes increasingly poorly damped as the forward speed increases; and, therefore, we expect that any variation of the handling qualities with flight condition should show up most strongly on the lateral outputs, i.e., in roll and heading. In addition, since the nominal roll and heading bandwidths are higher than the nominal pitch bandwidth, we would expect the match between the nominal and actual bandwidths to be best on the pitch channel because of the tendency of model error to increase with increasing frequency. Both of these expectations are confirmed by the values of the predicted bandwidths given in Table 1. The pitch bandwidths come out close to their design value of 2.5 rad/s and show little variation with flight condition, whereas the roll and heading bandwidths have come out to be a little greater than their nominal values and are more scattered.

Figure 4 shows the scaled step responses to pilot input on all four outputs for the 30-kt evaluation model. The height rate response is of the required delayed-first-order type. The pitch,

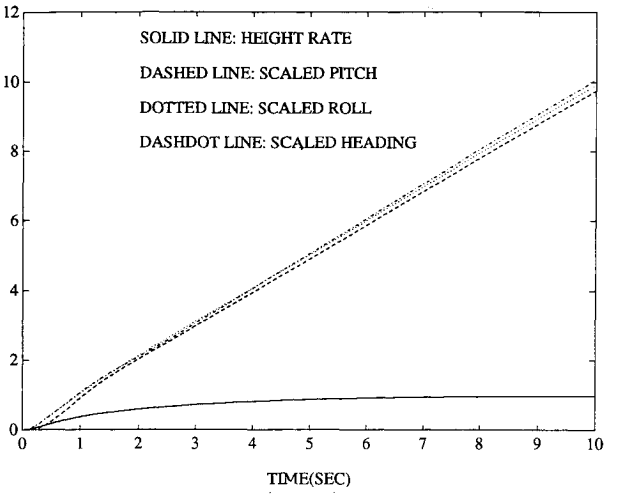

Fig. 4 Scaled on-axis step responses of 30-kt closed-loop system.

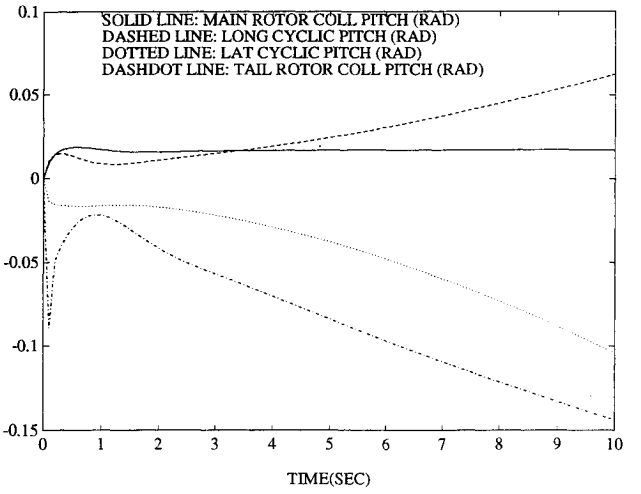

Fig. 5 On-axis control action for the step responses of Fig. 4.

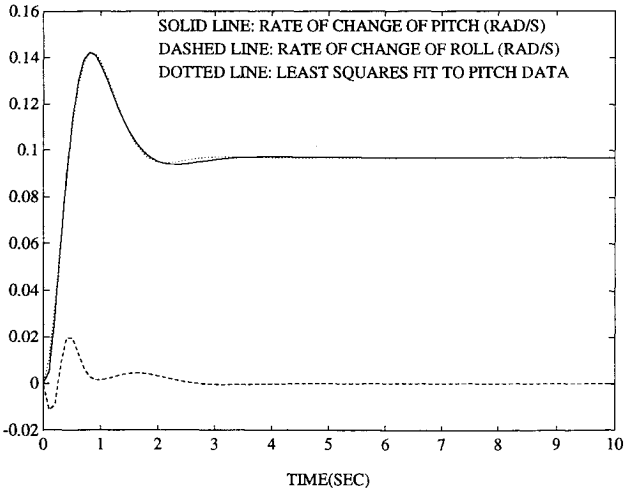

Fig. 6 Pitch rate and roll rate response for 0.1-rad/s pitch rate command at 30 kt.

Fig. 7 Scaled pitch to scaled roll coupling without shaping filter.

roll, and heading responses are, clearly, of the rate command type. Only the on-axis responses are shown in this figure. Figure 5 shows the corresponding on-axis control deflections, i.e., the main rotor collective pitch action for a 10-ft/s step, the longitudinal cyclic pitch action for a 0.1-rad/s step, and so on.

Figure 6 shows the rates of change of pitch and roll following a 0.1-rad/s pitch rate command applied to the 30-kt evaluation model. Also shown on the same axes are the least squares fit to the pitch rate response used to determine the effective damping factor. It can be seen that the curve of best fit matches the actual pitch rate response well. The parameters of the least squares fit were $\omega_n = 3.45$ rad/s, $\zeta = 0.60$, $a = 0.80$ s, $b = 0.097$, and $c = 0.36$ s. The large overshoot is seen to be due to a low-frequency effective zero at $1/a = 1.25$ rad/s. The underlying damping meets the specification easily.

As stated earlier, the version of the pitch-to-roll coupling requirement given in Hoh et al.[10] appears to be more readily applicable to rate command response types than the revised version in Ref. 1. In the former case the pitch-to-roll coupling is defined as the maximum roll rate obtained following a unit pitch rate command. The value for the 30-kt evaluation model (Fig. 6) is 0.21, and the values for all of the evaluation models are given in Table 1. It can be seen that the coupling is below the level 1/level 2 boundary, but that in the worst case at 50 kt, the coupling is only just at level 1. In view of this observation, it is worthwhile considering how the pitch-to-roll coupling could be improved. Figure 7 shows the magnitude of the scaled pitch-to-scaled roll transfer function for the open-loop system $G(s)K(s)$ and for the closed-loop system without the shaping filter, using the 30-kt evaluation model. Figure 7 makes it very clear that the problem originates in the frequency range immediately above the gain crossover frequency at 4.0 rad/s, where the benefits of the feedback have been largely lost, and before $G(s)K(s)$ has rolled off significantly. One approach would be to use a higher gain crossover frequency for the feedback loop; this might imply a need for a more accurate design model. A second approach would be to use a design method that gives the designer more control over the loop shape beyond crossover.[4] A third approach would be to use crossfeeds within the shaping filter. The disadvantage of the second and third approaches in this case is that they would amount to using open-loop control so that gain scheduling would almost certainly be necessary to take account of the variation of the plant dynamics with flight speed.

Summary and Conclusions

This paper has presented a control law design for low-speed flight of a typical combat rotorcraft. The specifications were based on a subset of the U.S. Army military rotorcraft handling qualities requirements. The design was based on the 30-kt linearized rigid-body model, together with a simplified representation of high-frequency effects. The design of the feedback loop used the LQG/LTR method with loop breaking at the plant output. The control law incorporated a form of integral action by using colored process noise within the linear quadratic Gaussian formalism. Numerical optimization was found to be an effective way of choosing the numerical values of the linear quadratic weighting parameters to fine tune the (asymptotic) loop shape. The detailed specifications for height rate and angular response provided guidance for the design of shaping filters outside the feedback loop. Evaluation of the designs was performed using a set of five high-order linearized models incorporating more accurate representations of actuators and rotors, and spanning the speed range from 10–50 kt at 10-kt intervals. It was found that all of the specifications could be met over this speed range without gain scheduling of the controller.

More formal loop shaping schemes (e.g., Safonov et al.[14]) can be used at the possible cost of a large increase in the order of the compensator associated with the frequency dependent weights on the various sensitivity functions. The design presented here meets its objectives with the relatively small increase in compensator order associated with the colored process noise.

It is concluded that the LQG/LTR framework is a useful tool for the preliminary linear design of helicopter flight control systems.

Appendix: Supplementary Data

The state space representation of the 30-kt linearized rigid-body helicopter model has input vector $\boldsymbol{u}$, state vector $\boldsymbol{x}$, and output vector $\boldsymbol{y}$ where

$$\boldsymbol{u} = \begin{bmatrix} \text{collective pitch, rad} \\ \text{longitudinal cyclic pitch, rad} \\ \text{lateral cyclic pitch, rad} \\ \text{tail rotor collective pitch, rad} \end{bmatrix} \tag{A1}$$

$$\boldsymbol{x} = \begin{bmatrix} \text{forward velocity, ft/s} \\ \text{vertical velocity, ft/s} \\ \text{pitch rate, rad/s} \\ \text{pitch angle, rad} \\ \text{lateral velocity, ft/s} \\ \text{roll rate, rad/s} \\ \text{roll angle, rad} \\ \text{yaw rate, rad/s} \\ \text{heading angle, rad} \end{bmatrix} \tag{A2}$$

$$\boldsymbol{y} = \begin{bmatrix} \text{height rate, 10 ft/s} \\ \text{pitch, 0.1 rad} \\ \text{roll, 0.2 rad} \\ \text{heading, 0.2 rad} \end{bmatrix} \tag{A3}$$

Note that the four components of $\boldsymbol{u}$ are already in the same units and it was not felt necessary to scale them. Given next are the rigid body A, B, and C matrices, the time delay dynamics (given in compact form),

$$\begin{bmatrix} A & B \\ C & D \end{bmatrix}$$

the Kalman filter gain matrix K_{lqe}, and the transpose of the LQR feedback matrix K_{lqr}. The structure of the shaping filter and the numerical values of its parameters are given in the main body of the text. Note that when the time delay model and the rigid body model are combined, the time delay state vector should make up the first four components of the composite state vector.

Rigid-body A matrix:

$$\begin{bmatrix}
-0.0098 & 0.0305 & -1.1774 & -32.1188 & -0.0118 & -0.4597 & 0 & 0 & 0 \\
-0.1632 & -0.5333 & 51.2195 & -2.0858 & -0.0172 & -0.4941 & 1.3028 & 0 & 0 \\
0.0110 & 0.0058 & -2.0510 & 0 & 0.0114 & 0.4320 & 0 & 0 & 0 \\
0 & 0 & 0.9992 & 0 & 0 & 0 & 0 & 0.0406 & 0 \\
0.0143 & 0.0189 & -0.4348 & 0.0847 & -0.0816 & 1.0326 & 32.0923 & -49.7509 & 0 \\
0.0099 & 0.0953 & -2.2384 & 0 & -0.0658 & -10.8462 & 0 & -0.1203 & 0 \\
0 & 0 & -0.0026 & 0 & 0 & 1.000 & 0 & 0.0649 & 0 \\
-0.0097 & 0.0129 & -0.3133 & 0 & 0.0101 & -1.8855 & 0 & -0.6791 & 0 \\
0 & 0 & -0.0406 & 0 & 0 & 0 & 0 & 1.0013 & 0
\end{bmatrix}$$

Rigid-body B matrix:

$$\begin{bmatrix}
16.7883 & -28.6070 & 6.6517 & 0 \\
-298.3142 & -30.1066 & 0.0023 & 0 \\
5.5417 & 26.8395 & -5.7691 & 0 \\
0 & 0 & 0 & 0 \\
2.2574 & -6.3561 & -30.5836 & 15.9209 \\
21.2054 & -31.6321 & -153.5206 & -0.9705 \\
0 & 0 & 0 & 0 \\
16.3444 & -5.8468 & -27.3854 & -13.0709 \\
0 & 0 & 0 & 0
\end{bmatrix}$$

Rigid-body C matrix:

$$\begin{bmatrix}
0.0065 & -0.0997 & 0 & 5.0666 & 0.0040 & 0 & -0.0133 & 0 & 0 \\
0 & 0 & 0 & 10.0000 & 0 & 0 & 0 & 0 & 0 \\
0 & 0 & 0 & 0 & 0 & 0 & 5.0000 & 0 & 0 \\
0 & 0 & 0 & 0 & 0 & 0 & 0 & 0 & 5.0000
\end{bmatrix}$$

State space model of time delays (compact form):

$$\begin{bmatrix}
-31.2500 & 0 & 0 & 0 & 1.0000 & 0 & 0 & 0 \\
0 & -14.4928 & 0 & 0 & 0 & 1.0000 & 0 & 0 \\
0 & 0 & -17.0940 & 0 & 0 & 0 & 1.0000 & 0 \\
0 & 0 & 0 & -54.0541 & 0 & 0 & 0 & 1.0000 \\
62.5000 & 0 & 0 & 0 & -1.0000 & 0 & 0 & 0 \\
0 & 28.9855 & 0 & 0 & 0 & -1.0000 & 0 & 0 \\
0 & 0 & 34.1880 & 0 & 0 & 0 & -1.0000 & 0 \\
0 & 0 & 0 & 108.1081 & 0 & 0 & 0 & -1.0000
\end{bmatrix}$$

Kalman filter gain matrix K_{lqe}:

$$\begin{bmatrix}
0 & 0 & 0 & 0 \\
-0.0000 & 0.0000 & 0.0000 & -0.0000 \\
-0.0000 & 0.0000 & -0.0000 & 0.0000 \\
0 & 0 & 0 & 0 \\
-0.2854 & -3.4745 & -0.3703 & 0.1592 \\
-33.1069 & 18.3339 & 4.4712 & -1.7578 \\
0.0045 & 0.7311 & 0.0487 & -0.1253 \\
0.0182 & 0.3820 & 0.0193 & -0.0095 \\
0.1673 & 0.0863 & 5.9606 & -37.1060 \\
-0.1848 & 0.0461 & 1.2838 & 0.0170 \\
-0.0329 & 0.0089 & 0.7094 & 0.0053 \\
-0.0279 & 0.0173 & -0.2909 & 1.4563 \\
-0.0088 & -0.0176 & 0.0212 & 0.7647 \\
-75.9293 & 3.0234 & 7.0101 & -0.2103 \\
0.1433 & 1.8824 & -0.3768 & -0.0630 \\
0.6986 & 0.5693 & 14.1276 & -1.8186 \\
0.0498 & 0.1211 & 1.1455 & 2.2661
\end{bmatrix}$$

Transpose of linear quadratic regulator gain matrix K_{lqr}:
$1.0e+03\times$

$$\begin{bmatrix}
1.8972 & 0.0999 & -0.1541 & -0.1286 \\
0.3249 & 1.2816 & 0.2550 & 0.0285 \\
-0.1939 & 0.0747 & 2.0136 & 0.2601 \\
-0.0052 & 0.0042 & 0.0227 & 0.1996 \\
0.0002 & -0.0000 & 0.0000 & 0.0000 \\
-0.0030 & 0.0005 & -0.0004 & -0.0001 \\
0.0073 & 0.0409 & -0.0052 & -0.0011 \\
0.2195 & 0.2752 & -0.0378 & -0.0165 \\
0.0001 & 0.0000 & 0.0001 & 0.0000 \\
0.0008 & -0.0019 & -0.0115 & 0.0003 \\
0.0135 & -0.0326 & -0.1538 & -0.0090 \\
0.0005 & -0.0001 & -0.0003 & -0.0105 \\
0.0037 & -0.0108 & 0.0118 & -0.1573 \\
-0.0002 & 0.0000 & -0.0000 & -0.0000 \\
0.0007 & 0.0032 & -0.0003 & -0.0001 \\
0.0000 & -0.0002 & -0.0008 & -0.0000 \\
0.0000 & 0.0000 & 0.0000 & -0.0004
\end{bmatrix}$$

Acknowledgments

I should like to thank D. J. Murray-Smith for his detailed and helpful comments on an earlier version of this paper. I should also like to thank DRA (Bedford) for the use of HELISTAB data and the "Handling Qualities Toolbox" which was used to calculate many of the handling qualities measures.

References

[1]Anon., "Aeronautical Design Standard, Handling Qualities for Military Rotorcraft," United States Army Aviation Systems Command, ADS-33C, St. Louis, MO, Aug. 1989.

[2]Garrard, W. L., Low, E., and Bidian, P. A., "Achievement of Rotorcraft Handling Qualities Specifications via Feedback Control," *Proceedings Sixteenth European Rotorcraft Forum* (Glasgow, Scotland, UK), Royal Aeronautical Society, London, 1990, pp. III.5.1.1-III.5.1.10.

[3]Walker, D., and Postlethwaite, I., "Full Authority Active Control System Design for a High Performance Helicopter," *Proceedings Sixteenth European Rotorcraft Forum* (Glasgow, Scotland, UK), Royal Aeronautical Society, London, Sept. 1990, pp. III.3.2.1-III.3.2.14.

[4]Stein, G., and Athans, M., "The LQG/LTR Procedure for Multivariable Feedback Control Design," *IEEE Transactions*, Vol. AC-32, No. 2, 1987, pp. 105-114.

[5]Maciejowski, J. M., *Multivariable Feedback Design*, Addison-Wesley, Reading, MA, 1989, Chap. 5, pp. 222-263.

[6]McLean, D., *Automatic Flight Control Systems*, Prentice-Hall, Englewood Cliffs, NJ, 1990, Chap. 13, pp. 451-490.

[7]Padfield, G. D., "A Theoretical Model of Helicopter Flight Mechanics for Application to Piloted Simulation," RAE-TR-81048, HMSO, London, 1981.

[8]Tischler, M. B., "Digital Control of Highly Augmented Combat Rotorcraft," NASA TM 88346, USAAVSCOM TR 87-A-5, May 1987.

[9]Hofmann, L. G., Riedel, S. A., and McRuer, D., "Practical Optimal Flight Control System Design for Helicopter Aircraft (Vol. 1—Technical)," NASA CR 3275, May 1980.

[10]Hoh, R. H., Mitchell, D. G., Aponso, B. L., Key, D. L., and Blanken, C. L., "Proposed Specification for Handling Qualities of Military Rotorcraft—Vol. 1: Requirements," NASA TM, USAAVSCOM TR 87-A-4, May 1988.

[11]Doyle, J. C., and Stein, G., "Multivariable Feedback Design: Concepts for a Classical/Modern Synthesis," *IEEE Transactions*, Vol. AC-26, No. 1, 1981, pp. 4-16.

[12]Kreindler, E., "On the Linear Optimal Servo Problem," *International Journal of Control*, Vol. 9, No. 4, 1969, pp. 465-472.

[13]Friedland, B., *Control System Design: An Introduction to State Space Methods*, McGraw-Hill, New York, 1987, Chap. 4, pp. 174-184.

[14]Safonov, M. G., Laub, A. J., and Hartmann, G. L., "Feedback Properties of Multivariable Systems: The Role and Use of the Return Difference Matrix," *IEEE Transactions*, Vol. AC-26, No. 1, 1981, pp. 47-65.